

The Final Remnant of Binary Black Hole Mergers: Multipolar Analysis

Robert Owen

*Center for Radiophysics and Space Research, Cornell University, Ithaca, NY 14853**

(Dated: September 24, 2009)

Methods are presented to define and compute source multipoles of dynamical horizons in numerical relativity codes, extending previous work in the isolated and dynamical horizon formalisms to allow for horizons that are not axisymmetric. These methods are then applied to a binary black hole merger simulation, providing evidence that the final remnant is a Kerr black hole, both through the (spatially) gauge-invariant recovery of the geometry of the apparent horizon, and through a detailed extraction of quasinormal ringing modes directly from the strong-field region.

PACS numbers: 04.25.D-,04.20.Cv,04.25.dg,04.30.Db

I. INTRODUCTION

The problem of the merger of binary black hole systems now seems to be well under the control of numerical relativity. More precisely, the development, due to Einstein's vacuum evolution equations, of an initial data set containing two apparent horizons into a quiescent state containing only one apparent horizon, has now been carried out numerous times by various research groups, with somewhat different numerical treatments and mathematical formalisms [1–4]. Numerical relativity is now a tool for studying the physics of strong gravitational fields.

When applying this tool, one is immediately faced with a fundamental irony of numerical relativity: a numerical code is incapable of dealing with abstract tensors, and must instead compute their components in a particular vector basis. The fundamental physics of general relativity, however, is basis independent. One must be careful to ensure that any physical claims are independent (to whatever extent is possible) of the coordinate system and vector basis in which they are demonstrated.

One reasonably well-developed example is the computation of spin angular momentum in binary black hole simulations. Numerous investigations have been made of the physics of spinning black hole mergers, presenting in some detail effects such as a hang-up of the merger, allowing angular momentum to be radiated so that the final remnant has sub-extremal spin [5]; spin flips [6], in which the dynamics of the merger cause the spin direction of the merged black hole to be dominated by the direction of orbital angular momentum, rather than the spins of the progenitor black holes; and perhaps of most astrophysical interest, the kick applied to a merged black hole system, balancing the linear momentum given off in gravitational radiation during nonsymmetric mergers [7–20]. A certain amount of investigation has also gone into the study of black holes of nearly-extremal spin in binary configurations, an avenue that could probe the limits of cosmic censorship [21, 22]. Because such physical effects must be parametrized according to the spin angular momenta

of the dynamical black holes, methods must be devised to define and compute such a quantity. The most common approach begins with a formula that appears both in the quasilocal formalism of Brown and York [23] and in the isolated and dynamical horizon formalisms [24, 25]. This formula gives angular momentum within a two-surface (normally taken to be an apparent horizon of spherical topology) as a functional of a vector field tangent to that surface. This vector field is interpreted as a generalized rotation generator, and it is through this that the vectorial nature of angular momentum in Newtonian mechanics is generalized. In order to apply this formula, a rule must be given for choosing such a generalized rotation generator on a dynamical black hole. Methods have recently been presented to fix these vector fields as “approximate Killing vectors” in a precise sense [22, 26–29].

The method presented in Refs. [22, 28, 29] actually provides much more information than just the generalized rotation generators. The method starts with the expression of the vector field in terms of a scalar potential:

$$\phi^A = \epsilon^{AB} \nabla_B z, \quad (1)$$

where uppercase latin letters index the tangent bundle to the two-dimensional surface, ∇ is the covariant derivative on this tangent bundle, inherited from that on spacetime, and ϵ_{AB} is the Levi-Civita tensor on the surface. The vector $\vec{\phi}$ is said to be an approximate Killing vector if it is of this form and if the function z satisfies a certain generalized eigenvalue problem on the surface. On a metric sphere¹, the operator in this problem reduces to the conventional spherical Laplacian, so these functions can be interpreted as spherical harmonics of the two-surface. In this special case, the three $\ell = 1$ harmonics provide the three standard rotation generators.

The appearance of generalized spherical harmonics in this formalism raises the possibility that one could naturally define more than just the spin angular momen-

*Electronic address: owen@astro.cornell.edu

¹ Throughout this paper, by “metric sphere” we mean a sphere in the metric sense: a closed 2-surface of constant positive intrinsic curvature, sometimes also referred to as a “round sphere.”

tum (which is often physically understood as the current dipole moment of the source). Perhaps with the help of the remaining eigenfunctions, we could define higher multipole moments.

The idea of quasilocal *source multipoles* in general relativity is not new. In Ref. [30], a complete formalism was presented for application on axisymmetric isolated horizons. This formalism involves numbers I_n and L_n , where n is a nonnegative integer index. Ashtekar et al. not only provided definitions for these multipole moments, they also proved that they completely characterize the isolated horizon geometry, that a unique isolated horizon (up to diffeomorphism) can be constructed from given multipole moments.

A few years later, Schnetter, Krishnan, and Beyer [31] were the first to apply this multipole moment formalism in numerically generated dynamical spacetimes. Their work was intended as a wide overview of the use of the dynamical horizon formalism in interpreting numerical relativity simulations; for them, multipole moments were just one of many points of discussion. They applied the formalism of [30] in an essentially unmodified form. Because this construction is restricted to axisymmetric horizons, the authors of [31] focused attention on an axisymmetric black hole merger.

Another application of this method appeared in Ref. [32], a paper presenting methods to solve for conformally curved initial data sets. As one might expect, when solving for a fully stationary single-black-hole initial data set, the result is a slice of the Kerr spacetime, a fact that the authors confirm using the multipole construction of Ref. [30].

Quite recently, another paper appeared [33] which introduced a novel scheme for computing multipole moments indirectly, from surface integrals of various powers of the curvature. This new method is still restricted to axisymmetric horizons, but it avoids the need to explicitly find the axisymmetry, and could markedly improve accuracy in cases where it can be used.

Here, we take a slightly different approach. Rather than directly applying the methods of Ref. [30] in an axisymmetric merger, we modify the method, in a manner briefly suggested by its authors, so that it can be applied without the requirement of axisymmetry. Whereas the original method in Ref. [30] involved a preferred coordinate system on the axisymmetric horizon, in which spherical harmonic projections could be taken, we choose to project the relevant quantities against spectrally-defined spherical harmonics. Such harmonics are invariantly defined on any given topological sphere endowed with intrinsic geometry, as eigenfunctions of geometric operators, such as the one mentioned above relevant to the computation of spin angular momentum. Extra structure, such as the axisymmetry that provides the preferred coordinate system of Ref. [30], is not necessary. While the continuum eigenvalue problems that define these harmonics would complicate analytical treatments, they are quite straightforward to solve numerically.

In section II we introduce the details of this method, in particular the eigenvalue problems used to define spherical harmonics on deformed spheres. In section III, we investigate one of the simplest applications of current physical relevance. This is the question of the final remnant of a numerical merger of two vacuum black holes. While the general expectation is that the remnant of such mergers will generically be a Kerr black hole, relatively little effort has gone into a detailed investigation of whether this is actually the case. This question is of relevance to the status of black hole uniqueness, whose rigorous proof still involves certain analyticity assumptions [34]. It is also related to the question of stability of the Kerr solution, which has so far been proven only for individual modes of linear perturbations [35]. Even if we fully accept the expectation that general relativity must force the remnant of a black hole merger to be Kerr, the detailed recovery of the Kerr solution at late times, in as gauge-invariant a manner as possible, provides at the very least a stringent and physically-relevant code test. In Ref. [36], Campanelli et al. demonstrated that a particular black hole merger simulation approaches Petrov type D in a certain sense at late times, and carries no NUT charge. This fact largely confirms that their merger produces a Kerr geometry. One advantage of their approach is that it is fully local, that one can investigate the approach to Kerr geometry throughout the spatial slices, rather than simply on the horizon as we do here. In a followup to the current paper, we intend to repeat many of the methods of Ref. [36] on the datasets discussed in Sec. III. Here we focus on multipole moments partly as a complementary method of black hole characterization, but also because these moments are of interest in their own right, as tools for probing the physics of tidal structure in strong-field gravity.

II. GENERALIZED SPHERICAL HARMONICS

The definitions given in Ref. [30] for the mass and current multipoles on isolated horizons are very simple spherical harmonic projections of quantities related to the intrinsic and extrinsic geometry of the apparent horizon² in spacetime.

$$I_\alpha := \oint y_\alpha R \, dA, \quad (2)$$

$$L_\alpha := \oint y_\alpha^B \omega_B \, dA. \quad (3)$$

Here, dA refers to the metric volume element on the apparent horizon, R is its intrinsic scalar curvature (not to

² In the case of isolated horizons, the surfaces of interest are arbitrary two-dimensional spacelike slices of the three-dimensional null isolated horizon. In the case of dynamical horizons, the two-surfaces of interest are the apparent horizons into which the dynamical horizon is naturally foliated.

be confused with the Ricci scalar of the full spacetime, or of the spatial slice, or of the horizon worldtube), and ω_A is a connection on the normal bundle of the two-surface, which is conveniently written in terms of the two future-directed null normals, $\vec{\ell}$ and \vec{n} :

$$\omega_A := e_A^\mu n_\nu {}^{(4)}\nabla_\mu \ell^\nu, \quad (4)$$

where ${}^{(4)}\nabla$ is the metric-compatible torsion-free spacetime covariant derivative, and $\{\vec{e}_A\}$ are basis vectors tangent to the two-surface. Throughout this paper, capital latin letters will index this two-dimensional tangent bundle. The null normals $\vec{\ell}$ and \vec{n} are, as usual, normalized such that $\vec{\ell} \cdot \vec{n} = -1$. In most numerical papers and codes, ω_A is written and computed in terms of the extrinsic curvature of the spatial slice. Here, we will refer to the I_α as the *mass multipoles* and the L_α as the *current multipoles*, though as noted in Ref. [30] extra factors involving horizon areas and quasilocal spins must be included if one wishes to make them dimensionally consistent with the standard definitions of these quantities.

The objects y_α appearing in (2) and y_α^A appearing in (3) are scalar and vector spherical harmonics, respectively. It is in the definition of these harmonics that the breaking of axisymmetry has the most immediately apparent cost, and therefore where the work in this paper will depart most strongly from the construction in Ref. [30]. In that paper, attention is focused on the case of axisymmetric isolated horizons. Axisymmetry provides a natural coordinate system on the apparent horizon, so the spherical harmonics used in Ref. [30] are the standard ($m = 0$) ones of spherical coordinates, applied in this canonical coordinate system. In other words, they are eigenfunctions not of the geometric Laplacian on the apparent horizon, but rather of the Laplacian of a metric sphere in these coordinates. There is nothing inherently wrong with such a choice in axisymmetry, in fact it provides certain benefits in that context³, but for purposes of strongly dynamical, strongly non-axisymmetric systems a more general approach is called for.

A. Scalar Spherical Harmonics

Our approach will be to define the spherical harmonics spectrally, as eigenfunctions of the geometric Laplacian operator (or certain generalizations thereof) on the apparent horizon surface. In other words, our scalar spherical harmonics are taken to be the functions y_α that satisfy the equation

$$\Delta y_\alpha = \lambda_{(\alpha)} y_\alpha \quad (5)$$

for some constant, $\lambda_{(\alpha)}$. The function y_α is defined only on the apparent horizon, and Δ is the intrinsic Laplacian of the apparent horizon, $\Delta := g^{AB} \nabla_A \nabla_B$. The letter α is a label for the various solutions to the eigenproblem.

Because the Laplacian in (5) reduces to the standard spherical Laplacian when the surface becomes a metric sphere, the functions y_α reduce to the standard spherical harmonics in that special case as well. However, this is not the only self-adjoint operator with this property. For example, we can consider the problem:

$$\Delta y_\alpha + q R y_\alpha = \lambda_{(\alpha)} y_\alpha, \quad (6)$$

where R is again the intrinsic scalar curvature of the surface and q is a numerical parameter. In the case of a metric sphere, where R is constant, the second term on the left side does not alter the eigenfunctions, it merely increases each eigenvalue. This eigenproblem, therefore, can again be considered to define a reasonable generalization of coordinate spherical harmonics. However, on a deformed sphere, where R is not constant, these generalized spherical harmonics will no longer agree with those defined by (5). To fix this arbitrariness, and since we see no particular reason to prefer any other value for q , we choose $q = 0$, in other words the problem in Eq. (5), to define our scalar spherical harmonics. In the case of vector spherical harmonics, we will see a geometrical reason to prefer a particular value for an analogous parameter.

B. Vector Spherical Harmonics

We will take our generalized vector spherical harmonics to be tangent to the surface, in which case they can be written in terms of gradients of two scalar potentials:

$$y_\alpha^A = \nabla^A w_\alpha + \epsilon^{AB} \nabla_B z_\alpha. \quad (7)$$

Here ∇ is the torsion-free metric-compatible derivative on the apparent horizon, and ϵ_{AB} is the Levi-Civita tensor on it. To consider the importance of these two potentials we should investigate the one-form ω_A against which the vector spherical harmonics will be projected. In Eq. (4), the future-directed null vectors $\vec{\ell}$ and \vec{n} are orthogonal to the apparent horizon and normalized relative to one another by the standard Newman-Penrose condition $\vec{n} \cdot \vec{\ell} = -1$, but are otherwise free. One can arbitrarily scale the $\vec{\ell}$ vector at the cost of inversely scaling the \vec{n} vector. This ‘‘boost freedom’’ is a standard gauge degree of freedom in the dynamical horizon formalism. The dynamical horizon worldtube carries with it a preferred slicing into apparent horizons, but this slicing is only of the dynamical horizon itself. There is no preferred way of extending this slicing into the ambient spacetime. If we wish for our horizon multipoles to be independent of this gauge freedom, then we must choose harmonics that project out only the gauge invariant part of ω_A .

³ One such benefit is that the mass dipole moment always turns out to be zero. In other words, their construction guarantees that one is in a ‘‘center of mass frame.’’ In general, this may not hold in our construction, though we have not yet seen an example where it fails.

From Eq. (4), it is apparent that a boost, $\vec{\ell} \mapsto a\vec{\ell}$, $\vec{n} \mapsto a^{-1}\vec{n}$, will add a pure gradient to ω_A :

$$\omega_A \mapsto \omega_A - \nabla_A \log(a). \quad (8)$$

Any part of ω_A that is a pure gradient is therefore entirely due to boost gauge, in the sense that it can be transformed away by an appropriate boost. Vector spherical harmonics of the form $y_\alpha^A = \nabla^A w_\alpha$ will pick up this gauge-dependent information in the integral (3), however vector spherical harmonics of the form $y_\alpha^A = \epsilon^{AB} \nabla_B z_\alpha$ will not. We therefore restrict all attention to vector spherical harmonics of this latter form.

We now need a rule to define the potential functions z_α that appear in these vector spherical harmonics. In the case of a metric sphere, the obvious choice is that they be the scalar spherical harmonics. As in the previous subsection, there are many ways to generalize the spherical harmonics of the metric sphere. For the current purposes, there is reason to prefer a somewhat complicated fourth-order generalized eigenproblem:

$$\Delta^2 z_\alpha + \nabla^A (R \nabla_A z_\alpha) = \lambda_{(\alpha)} \Delta z_\alpha. \quad (9)$$

This generalized eigenproblem also defines the potentials for the approximate Killing vector fields used for computing spin angular momentum in Ref. [22]. For this reason, when this problem is used to define the vector spherical harmonics, the current dipole moment of the horizon is identical to the quasilocal spin defined there, a quantity that itself reduces on axisymmetric isolated horizons to the quasilocal spin defined by Hamiltonian methods [24]. In Ref. [30], the agreement of the current dipole with the spin is cited as a reason to prefer using coordinate harmonics in a canonical coordinate system rather than spectrally-defined harmonics. There it was assumed that such harmonics would be simple eigenfunctions of the Laplacian, like the scalar spherical harmonics of the previous subsection, in which case the current dipole would not agree with the standard spin angular momentum. We have averted this situation simply by choosing a better operator.

We should also note that when vector spherical harmonics are chosen in this way, we are assured that there will be no current monopole moment. This fact can be viewed in a number of related ways. On the simplest level, there is the fact that when the vector spherical harmonics are defined to be of the form $y_\alpha^A = \epsilon^{AB} \nabla_B z_\alpha$, then a potential of the form $z_\alpha = \text{const.}$ cannot define a (normalizable) vector spherical harmonic. In some sense, $z_\alpha = \text{const.}$ can be viewed as a solution to Eq. (9) with arbitrary eigenvalue, but it is not a well-behaved solution. The generalized eigenproblem is technically *singular* in function spaces that include constants [37], meaning that well-behaved solutions cannot be found unless the function space is restricted to, for example, functions with zero average over the sphere, a condition which removes all nonzero constants from consideration.

Another way of looking at this, which helps to elucidate the relationship between the mass and current mul-

tipoles, is that when the vector spherical harmonics are defined in this way, an integration by parts allows the current moments to be written as:

$$L_\alpha := \oint z_\alpha \Omega \, dA, \quad (10)$$

where $\Omega := \epsilon^{AB} \nabla_A \omega_B$ can be interpreted geometrically as a scalar curvature of the normal bundle of the two-dimensional surface in four-dimensional spacetime. The current moments thus represent for the extrinsic geometry of the apparent horizon what the mass moments represent for its intrinsic geometry.

The complex combination of these two curvatures, $R + i\Omega$, is sometimes called the *complex curvature* of the two-surface embedding. As is briefly described in Sec. 4.14 of Ref. [38], the vanishing of the current monopole moment can be understood geometrically in this context as a result of the generalization of the Gauss-Bonnet theorem to the lorentzian normal bundle. The integral of any constant multiple of Ω is a topological invariant, just like that of R , but because the gauge group on the normal bundle is topologically trivial, this invariant must always vanish.

One final point to note, with regard to both the scalar and the vector harmonics, is that of normalization. Solutions of the eigenproblems in Eqs. (5) and (9) are determined only up to constant multiplicative factors⁴. We fix these factors with an integral normalization condition. The condition imposed on scalar spherical harmonics is:

$$\oint (y_\alpha)^2 \, dA = 1. \quad (11)$$

On metric spheres in Euclidean space, this reduces to the standard normalization condition for scalar spherical harmonics (up to a factor of areal radius).

For vector spherical harmonics, the normalization condition we impose is:

$$\oint g_{AB} y_\alpha^A y_\alpha^B \, dA = 1. \quad (12)$$

This differs slightly from the standard normalization condition for axial vector spherical harmonics in euclidean space, which involves an extra factor of $\ell(\ell + 1)$, but because the generalization of the index ℓ is not an integer, but rather a function of the eigenvalue $\lambda_{(\alpha)}$, we simply leave this factor out.

Normalization conditions like those above still don't determine a sign for the spherical harmonics. This sign ambiguity translates directly into a sign ambiguity for the multipoles. We fix the sign with the condition that the values of the multipole moments be nonnegative.

⁴ In fact, solutions of Eq. (9) are determined only up to constant multiplicative and additive factors, however additive constants have no effect on the multipoles due to the vanishing of the current monopole.

In summary, the approach we take to defining multipoles in numerical simulations begins with finding solutions y_α and z_α of the eigenproblems (5) and (9) defined on the apparent horizon two-surface. From the potential z_α , vector spherical harmonics are computed as $y_\alpha^A := \epsilon^{AB} \nabla_B z_\alpha$. The harmonics are normalized with the conditions in Eqns. (11) and (12). Then, the surface integrals in Eqns. (2) and (3) are computed to be the multipoles.

III. NUMERICAL RESULTS

The immediate purpose of this mathematical machinery is to investigate the remnant of a binary black hole merger. There is a very large space of physically-relevant mergers worth investigating, including variations in the initial mass ratio, eccentricity, spin magnitudes, and spin directions. For this paper we will focus on a very simple case: the merger of a non-eccentric binary of equal mass, nonspinning black holes. This data set is discussed in detail in Ref. [4], which briefly notes the fact that two independent measures of the final spin agree to well within their expected numerical errors. This claim can be considered a first indication that the tidal structure of the quiescent black hole is that of Kerr, as this is the case in which these two measures of spin are designed to agree. Our goal now is to present the rest of the tidal information, to the extent that it can be resolved in the code, to strengthen the case that the final remnant is a Kerr black hole.

The code used to compute these multipoles is a part of the Spectral Einstein Code (SpEC) developed and maintained by the Caltech and Cornell Numerical Relativity groups, particularly Lawrence E. Kidder, Harald P. Pfeiffer, and Mark A. Scheel. Once an apparent horizon has been found, using the method described in Ref. [39], the code interpolates all relevant data to a pseudospectral grid on that surface. Because this grid is pseudospectral, the code can automatically transform any smooth function on the apparent horizon into a truncated expansion in coordinate spherical harmonics. This expansion, inserted into Eq. (5) or (9), provides a finite-dimensional matrix eigenproblem (or generalized eigenproblem in the latter case) which is solved using the LAPACK routine `dggev`. We emphasize that while this construction involves coordinate spherical harmonics, they are only used to supply the numerical discretization, so they disappear in the continuum limit. The *geometrical* spherical harmonics y_α and y_α^A that define the multipoles are, apart from numerical truncation error, uniquely defined on any given two-sphere (up to possible degeneracy in the eigenspaces).

The information that we can assess includes not only the values of the multipole moments defined in Eqns. (2) and (3), but also the spectrum of eigenvalues in Eqns. (5) and (9). A particular motivation for investigating eigenvalues of geometric operators is that they provide an in-

dications of symmetries in the horizon. As is familiar from elementary quantum mechanics, a symmetry in an operator leads to degeneracies in its eigenspaces. The converse is not necessarily true, but on an intuitive level we may interpret degeneracies in the eigenspectrum as indicators of possible symmetry.

This is an interesting tool for the study of this particular problem, because in the ringdown after a nonspinning black hole merger there is a transition from one axis of symmetry to another. Immediately after the formation of a common apparent horizon, one intuitively expects this horizon to be “peanut shaped,” with an axis of approximate symmetry⁵ along a line connecting the previous two individual apparent horizons. After the ringdown is complete, one would expect a single black hole with symmetry about the axis of the initial orbital angular momentum. This breaking and forming of symmetries is demonstrated in Fig. 1. The figure presents the three eigenvalues of the horizon Laplacian associated with harmonics that would settle to the $\ell = 1$ spherical harmonics if the horizon were to become metrically spherical. Two of these curves overlap at early times, a degeneracy due to the approximate axisymmetry of the initial “peanut” shape. As this symmetry is broken during the ringdown, the degeneracy breaks and one eigenvalue eventually joins up with the third eigenvalue, demonstrating the eventual axisymmetry about the spin direction.⁶

With the next five eigenvalues, in Fig. 2, we see the pattern again. Again, modes are nearly degenerate at early times, but split off during the ringdown and reconnect as the quiescent symmetry is approached. Note, however, that one degeneracy at early times is quite visibly broken. This may be due, on an intuitive level, to the tidal interaction of the two black holes during inspiral, with shifted phase due to horizon viscosity [40–42]. Because such tidal interaction is a quadrupolar effect, it would make sense for it to be less visible in the dipolar information of Fig. 1.

Degeneracies in the other eigenproblem, Eq. (9), give a similar picture of the breaking and reforming of symmetries, but this problem gives an even more compelling picture of the relationship between symmetries and de-

⁵ In the case studied here, this axisymmetry would only be approximate, as tidal bulges would be expected to phase-shift due to horizon viscosity during the inspiral. In the case of a direct head-on collision of nonspinning holes, this axisymmetry would be exact, and would be preserved even through the ringdown.

⁶ All figures in this paper give quantities computed in code units evaluated with respect to coordinate time which is also expressed in code units. For context, the final black hole described in Figs. 1–9 has horizon mass $M \approx 1.98$ in these code units, where this mass is defined by the Christodoulou formula $M^2 = M_{irr}^2 + J^2/(4M_{irr}^2)$ where $M_{irr} = \sqrt{A/(16\pi)}$ is the irreducible mass and J is the quasilocal spin angular momentum defined in Appendix A of Ref. [22]. In the simulation presented in Figs. 10–13, the value of this final mass in code units is $M \approx 2.56$.

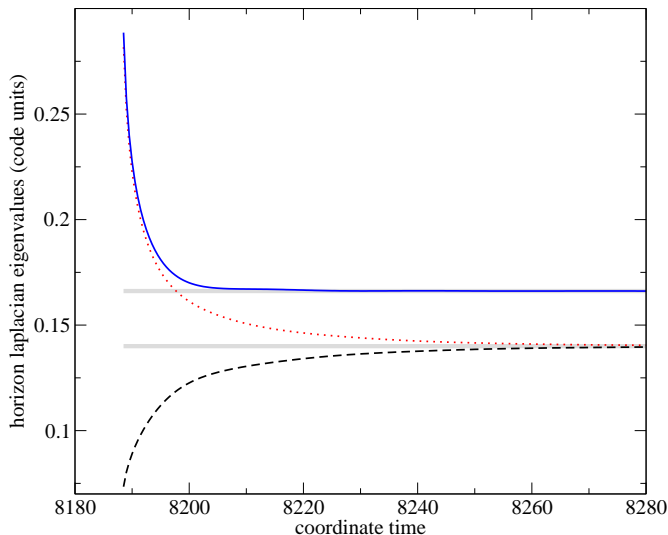


FIG. 1: Absolute values of the lowest three (dipole) nontrivial eigenvalues of the Laplacian on the dynamical horizon during the ringdown. The breaking away of the red (dotted) curve from the blue (solid) curve at early times is due to the breaking of the initial (approximate) “peanut” axisymmetry. The joining of this curve onto the black (dashed) curve at late times is due to the late-term axisymmetry of the final Kerr horizon. The horizontal gray lines represent the expected eigenvalues on a Kerr horizon with mass and spin equal to the final measured values in the simulation. Thus the convergence of the eigenvalues to these lines demonstrates the approach to Kerr geometry.

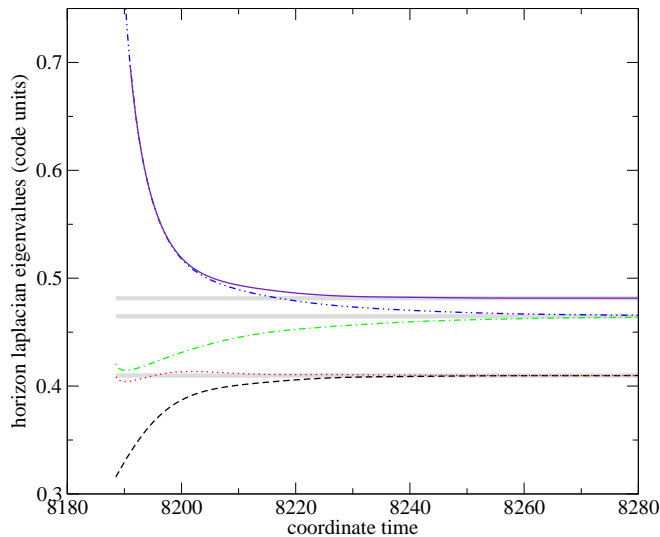


FIG. 2: Absolute values of the next five (quadrupole) eigenvalues of the Laplacian on the dynamical horizon during the ringdown. As in Fig. 1, the curves are paired up at early times, split their degeneracies, and connect in a different pairing at late times, again indicating transition from one axis of symmetry to another. The fact that one of these degenerate pairs at early times is visibly nondegenerate indicates imperfection in the “peanut” axisymmetry intuitively due to phase offset tidal bulges built up during the inspiral.

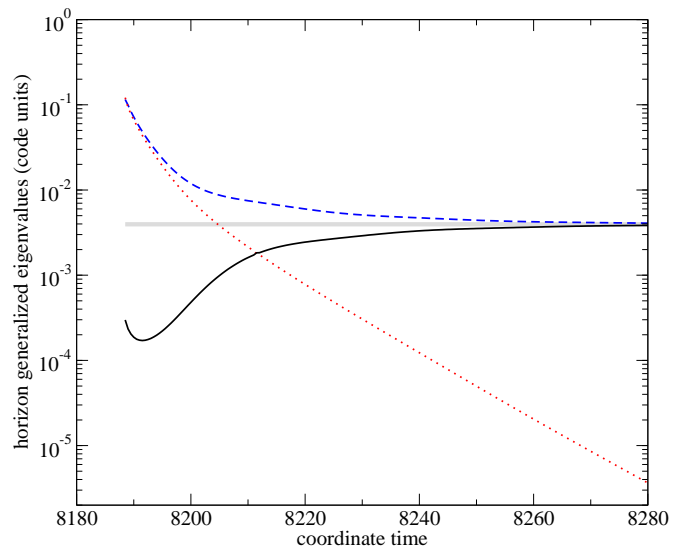


FIG. 3: Absolute values of the lowest three (dipole) nontrivial eigenvalues of the generalized eigenvalue problem in Eq. (9) on the dynamical horizon during the ringdown. The vertical axis is now scaled logarithmically to better show the approach of the smallest eigenvalue to zero. As argued in Appendix A of Ref. [22], the vanishing of this smallest eigenvalue is direct evidence of a rotational symmetry of the intrinsic surface geometry, so this figure provides a clear picture not only of the symmetry transition itself, but also of the relationship between symmetries and degeneracies. In particular, the crossing of the red and black (dotted and solid) curves can be seen as an example of “accidental” degeneracy, degeneracy that is not necessitated by a symmetry of the operators.

generacies. The original motivation of Eq. (9), as described in Appendix A of Ref. [22], was to construct, in a sense, the closest possible approximation of an axial symmetry on a horizon that may not have any true symmetries at all. One can easily show that the value of a given eigenvalue is proportional to the integral of the square of the residual in Killing’s equation for the associated “approximate Killing vector” field. Thus, when there is a true symmetry, and therefore a true Killing vector field, one of the eigenvalues of this problem will equal zero. So from plots of the eigenvalues of Eq. (9) we can see the breaking and forming of symmetries both indirectly, through degeneracies of the eigenspaces, and directly, through the value of the lowest eigenvalue. Figure 3 shows the three lowest eigenvalues of this problem. As noted at the end of Sec. II B, there are no monopole harmonics at all for this problem, so these are the three harmonics that would reduce to the $\ell = 1$ harmonics if the horizon approached a metric sphere. The vertical axis of the figure is now logarithmically scaled, to show the approach of the smallest eigenvalue to zero both at early and late times.

These figures also provide a quantitative picture of the intrinsic geometry of the apparent horizon, and its approach at late times to the geometry of a slice of the Kerr horizon. The horizontal lines in Figs. 1–3 represent

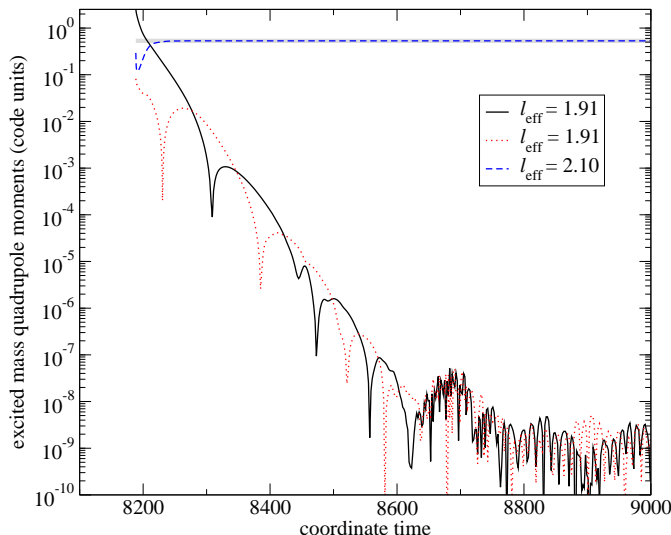


FIG. 4: Relaxation of the three excited quadrupole moments to expected Kerr values. Two of the five possible quadrupole moments must vanish due to the reflection symmetry in the problem, and indeed, their computed values are small enough to be considered zero to within ordinary numerical errors. Of the remaining three multipoles, two fall exponentially toward the level of numerical truncation, and the third quickly settles to the expected value for a Kerr black hole of the same final mass and spin. This expected value is shown in the thick horizontal gray line, which for most of the simulation overlaps the dashed blue curve. In this and later figures, curves are labeled by the “effective” ℓ values of their corresponding spherical harmonic at late times. That is, ℓ_{eff} is defined from the value of the eigenvalue λ at late times by the equation $\lambda = -\ell_{\text{eff}}(\ell_{\text{eff}} + 1)/r^2$, where r is the areal radius of the horizon, again measured after the hole settles down.

the expected values for these eigenvalues on a Kerr horizon of the same mass and spin as is measured at very late times in the simulation. Note that this spin is guaranteed to be identical to the late time current dipole moment on the horizon (this is the main motivation for Eq. (9)), so agreement of the current dipole with the “expected Kerr value” is trivial, however the consistency of all other multipoles, as well as these eigenspectra, present a nontrivial demonstration that the quiescent hole is Kerr.

Figures 4–8 present the behavior of the multipole moments. In Fig. 4, the three excited quadrupole moments are shown (the other two vanish as demanded by reflection symmetry). One moment starts out relatively small and grows to take the value expected for a Kerr black hole. The other two fall exponentially toward zero, until reaching the level of numerical truncation. Figure 5 shows the convergence of this floor of numerical error for three values of the resolution of the numerical simulation. On all three simulations, the horizon finder and eigenvalue solver are run at the maximum relevant resolution, essentially the same as the angular resolution of the original simulations. Figures 6–8 are analogous to Fig. 4, showing higher-order multipole moments. Again,

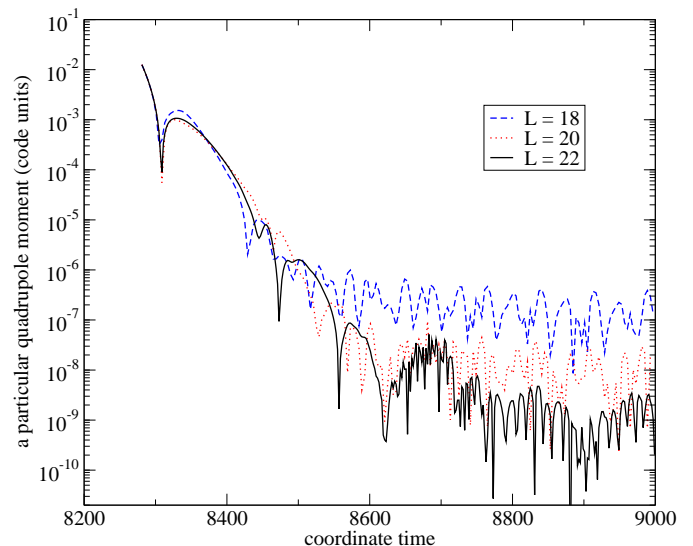


FIG. 5: A particular quadrupole moment from Fig. 4 shown for three different resolutions. The order of the pseudospectral angular discretization is given by $L = 18, 20, 22$ respectively, L representing the maximum ℓ -value of coordinate spherical harmonics used to discretize the problem. At late times, the exponential falloff halts, but the level where this occurs converges exponentially toward zero as L is increased. These nonzero values can therefore be attributed to standard truncation error.

all multipoles allowed by the reflection symmetry of the problem are excited near the moment of merger, but in each case a single moment rises to the expected value for a Kerr black hole of the measured final mass and spin, while all other multipoles decay exponentially toward zero before stopping due to numerical truncation.

The fact that those multipoles that decay to zero do so exponentially raises the question of whether this decay can be attributed to quasinormal ringing. The answer to this question is clouded by a few subtleties. For one, while the multipoles do appear to oscillate within an exponential envelope, this oscillation does not appear to be even approximately periodic, and at any rate occurs on a much longer timescale (compared to the exponential decay timescale) than the oscillations associated with quasinormal ringing. There is an intuitive explanation for this. Because the multipoles are defined with respect to spherical harmonics that are fixed by the intrinsic geometry of the horizon, changes in horizon geometry will cause changes in these harmonics. In particular, if the major part of the perturbation from Kerr geometry is a nonaxisymmetric bulge that rotates around the spin axis, then the spherical harmonics will be dragged along with this bulge. Intuitively, an ideal “ $\ell = 2, m = 2$ ” bulge would be expected to drag the spherical harmonics into corotation with it, so the multipole representing this bulge would be expected to fall off as a pure exponential, with no oscillation. In reality, the situation is more complicated, presumably due in part to the existence of

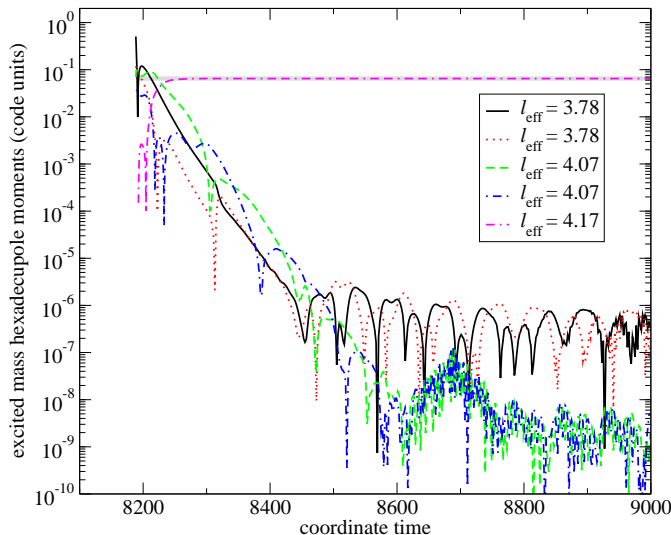


FIG. 6: Relaxation of the five excited hexadecupole mass moments to expected Kerr values. Four of the nine possible moments vanish due to the reflection symmetry in the problem. Of the remaining five, four fall to zero exponentially, and the other rises to the expected value for a Kerr black hole.

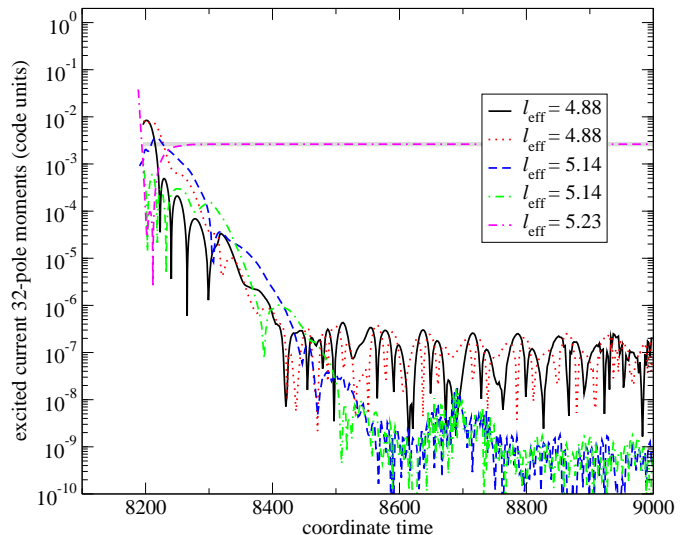


FIG. 8: Of the eleven current 32-pole moments, only five are allowed by the reflection symmetry to be excited. Again, four fall exponentially toward the level of numerical truncation error, and the other exponentially approaches its expected value for a Kerr hole. The quantity ℓ_{eff} labeling the curves is defined as in Fig. 7.

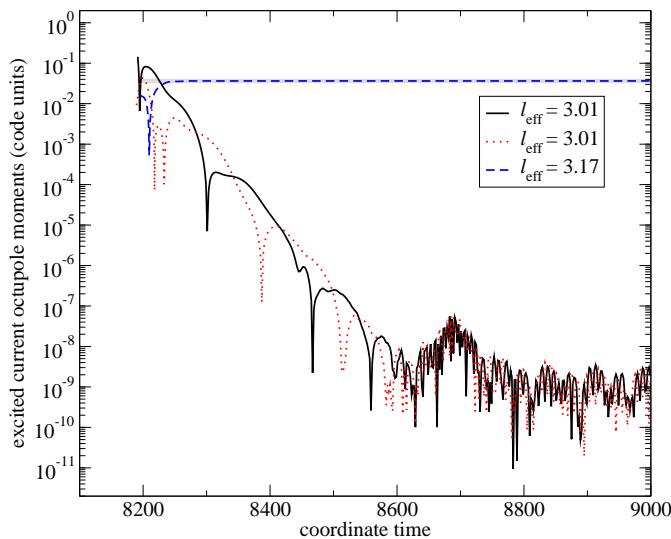


FIG. 7: Of the seven current octupole moments, only three are allowed by the reflection symmetry to be excited. Again, two fall exponentially toward the level of numerical truncation error, and the other exponentially approaches its expected value for a Kerr hole. The quantity ℓ_{eff} labeling the curves is again computed from the eigenvalue at late times, but the definition is now given by the equation $\lambda = -\ell_{\text{eff}}(\ell_{\text{eff}} + 1)/r^2 + 2/r^2$, taken from the special case of Eq. (9) on a round sphere.

higher multipolar structure, and in part due to the eventual approach to axisymmetry, causing degeneracies in the eigenproblems to be broken at the numerical level rather than at the analytical one.

Properly “unwinding” this rotation of the harmonics would amount to a partial fixing of angular coordinates.

There may be sensible ways to do this, but we consider this somewhat outside the scope of the current research, so instead we choose to ignore the oscillatory behavior, by focusing on the quadratic sums of multipoles associated with nearly-degenerate eigenspaces. In particular, the two exponentially-decaying curves in Fig. 4 are associated with such an asymptotically degenerate eigenspace, and can intuitively be interpreted as real and imaginary parts of the “ $\ell = 2, m = 2$ ” multipole. Their quadratic sum can therefore be viewed as the overall “magnitude” of the quadrupolar part of this rotating bulge, and would be expected to fall off exponentially in time without oscillation. Figure 9 shows the value of this quadratic sum as well as the falloff rate expected from perturbation theory. We used the method due to Leaver [43] to compute quasinormal frequencies in terms of the roots of two coupled complex continued fractions. For the mass and spin, we used values computed at late times on the horizon and reported in Ref. [4].

The remarkably fine agreement between this quadratic sum of multipole moments and the expected exponential falloff of the dominant “ $\ell = 2, m = 2$ ” quasinormal mode in perturbations of the Kerr geometry makes it tempting to try to pick other quasinormal ringing modes out of the data. This however would be a somewhat nontrivial undertaking. For one thing, all multipoles defined in our formalism are computed from data directly on the horizon. Different radial modes of black hole perturbations would be directly superposed in the multipoles. Further complicating matters in the case of a Kerr hole, the angular dependence of the quasinormal modes are not given by pure spherical harmonics, as defined here, but as solu-

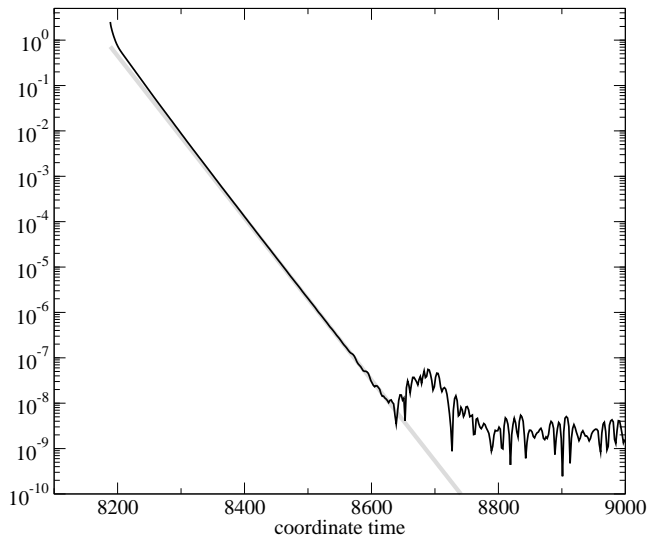


FIG. 9: The quadratic sum $Q(t) := \sqrt{q_1^2(t) + q_2^2(t)}$ of the two moments q_1 and q_2 that fall exponentially to zero in Fig. 4. The thick gray line shows the expected falloff of this quantity in perturbation theory.

tions of the “angular equation” of the Teukolsky formalism (Eq. (4.10) of Ref. [44]). Thus all multipoles would be expected to project out components of all radial and angular quasinormal modes, rather than cleanly projecting out one at a time. What is seen in Fig. 9 as exponential decay is actually just the dominant term of a multiexponential expansion. The problem of fitting data to a sum of exponentials is famously ill posed, so any effort to pick out higher-order ringing modes from this data would be quite ambitious, if possible at all.

Many of these complications disappear if the final black hole is nonspinning. In that case, the quasinormal modes should have the angular dependence of pure spherical harmonics, so multipoles of a given order can be expected to project out modes of the same order (though, again, multiple radial modes would be expected to overlap). Also, if there are enough degrees of reflection symmetry to forbid the rotation of the spherical harmonics described above, one might hope to recover not only the exponential falloff rates of different quasinormal modes, but also their frequencies of oscillation.

Figures 10–13 demonstrate this recovery. The data used here are from the ringdown after the collision of two black holes of nonzero antialigned spin (and therefore zero total angular momentum) starting from rest. This is a simple test case that can be used for studying black hole kicks, and the particular simulation studied here will be presented in great detail for that goal in an upcoming paper [45]. For the present purposes, the important points are that the final state is nonspinning, and that two orthogonal planes of reflection symmetry (the coordinate $x = 0$ and $z = 0$ planes, with the final kick being in the y direction) hold the harmonics in place, in that they remain symmetric or antisymmetric under the

action of the reflection symmetries. Figures analogous to Figs. 10–13 for the current multipoles show similar agreement, but are omitted here because they look essentially the same. Incidentally, similar (though less detailed) agreement with quasinormal ringing frequencies was noted in the oscillation of the area of spatial slices of the event horizon in other recent simulations using the SpEC code [46].

One subtlety with Figs. 10–13 must be noted. At late times, when these moments reach levels on the order of 10^{-9} , the data become quite noisy. This is a result of numerical errors, particularly the truncation error of the angular discretization. However it appears that the numerical data in Figs. 11–13 continue to decrease as the simulation goes on. This is an artefact of the manner in which the data are extracted. The numerical code computes essentially as many multipoles as there are grid points on the interpolated apparent horizon. These multipoles must be ordered in some way. The most obvious ordering is provided by the eigenvalues of the spherical harmonics. However such an ordering is not effective when families of eigenspaces are nearly degenerate, as particularly in the case of ringdown to a Schwarzschild black hole. To pick out particular eigenvalues in this quasinormal ringdown phase, we employ a simple post-processing script that chooses, at each timestep, the particular multipole moment that has value closest to a “prototype” value taken from the perturbation theory results shown in the red curves in these figures. Simultaneously, the script checks that any chosen multipole corresponds to an eigenvalue which lies within a certain range, so that the multipole is assured to have the proper “ ℓ ” value. After this searching is carried out, we check the eigenvalue, as a function of time, corresponding to the chosen multipole, to ensure that it is smooth and therefore that the procedure has chosen a consistent multipole and eigenvalue dataset⁷. This procedure nicely and unambiguously recovers physical perturbations during most of the ringdown. However at late times the perturbation is small enough that the ordering ambiguity is particularly strong. At late times, the script chooses the moment closest to the prototype value, out of the many that are oscillating quickly at small values due to numerical error, yet all eigenvalues in the given range are essentially the same, so the smoothness of the eigenvalue is no longer an effective tool to distinguish the correct moment from the others of the same ℓ . The matching of the numerical data to the prototype function is therefore given more weight than it deserves, and the data, though clearly flooded with numerical er-

⁷ Immediately after the formation of the common horizon, when deviations from the expectations of linearized theory are strongest, this script can again have trouble finding consistent multipole and eigenvalue datasets. For this reason some data are omitted from the beginning of Figure 12, as nonsmoothness of the eigenvalues showed that the chosen multipoles did not represent a consistent dataset at very early times.

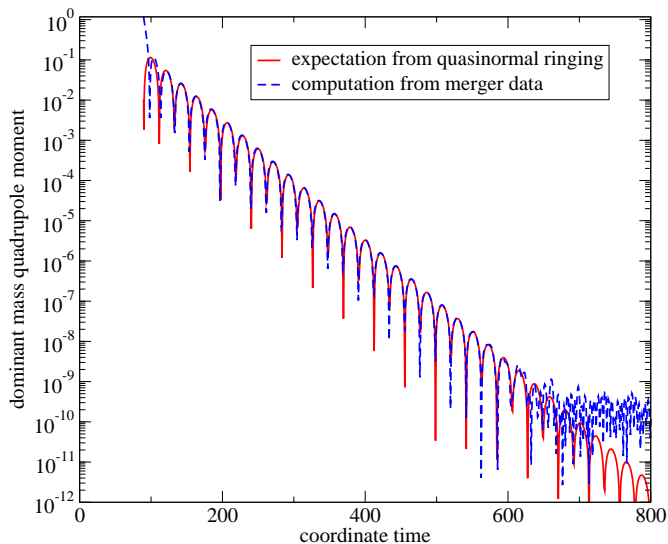


FIG. 10: Ringing of the dominant mass quadrupole moment as the product of a nonaxisymmetric head-on merger settles down to a Schwarzschild black hole. The dashed blue curve represents numerical data, and the solid red curve is an exponentially-damped sinusoid, with frequency and damping corresponding to quadrupole gravitational quasinormal modes of a Schwarzschild black hole [43]. An arbitrary constant amplitude scaling and phase have been applied to the red curve, by eye.

ror, continue to fall off exponentially in time. Figure 10 is an exception to this behavior. In that particular case, a method involving matching the spherical harmonics to coordinate spherical harmonics was able to unambiguously pick out the “correct” harmonic. For higher multipoles that method failed, apparently due to the rotation ambiguity of the coordinate spherical harmonics themselves.

The quality of the agreement with standard quasinormal ringing frequencies, both in the approach to Schwarzschild geometry in Figs. 10–13 and in the approach to Kerr geometry in Fig. 9, initially came as quite a surprise, considering that a major motivation for this project is a healthy skepticism for the quality of the coordinates in numerical simulations. While the slicings used here are not arbitrary — both simulations employ harmonic slicings during the ringdown, as do conventional treatments of black hole perturbation theory — they are nonetheless *different* harmonic slicings than those in conventional perturbation theory, because the ones used in our simulations are horizon-penetrating. One might ask, then, how the numerical code knows to settle on a harmonic slicing in which these frequencies come out as expected. The answer lies in the approach to stationarity. At late times the simulations develop approximate stationary Killing vector fields $\vec{\xi}$, and the coordinate components of the spacetime metric tensor asymptote to constant values, meaning that the coordinates adapt themselves to the symmetry such that $\vec{\partial}_t \rightarrow \vec{\xi}$. This turns the

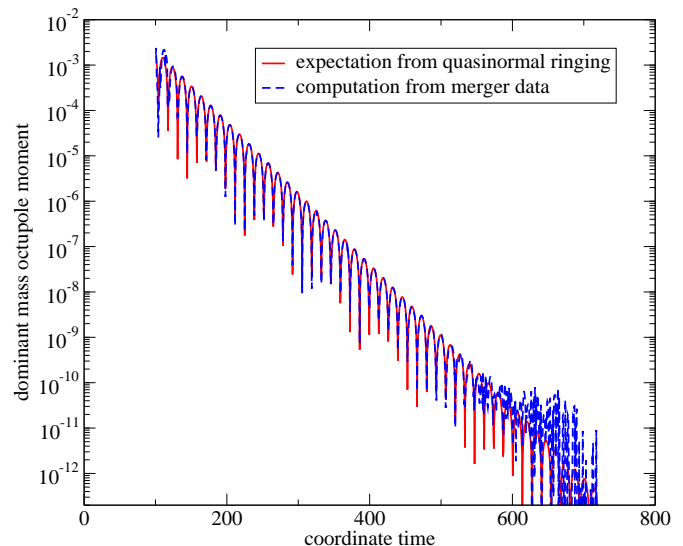


FIG. 11: Ringing of the dominant mass octupole moment as the product of a nonaxisymmetric head-on merger settles down to a Schwarzschild black hole.

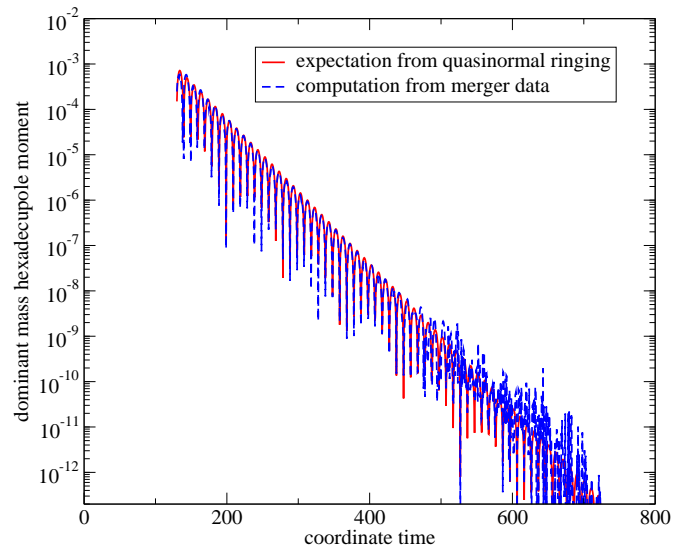


FIG. 12: Ringing of the dominant mass hexadecupole moment as the product of a nonaxisymmetric head-on merger settles down to a Schwarzschild black hole.

definition of the ringing frequencies into a geometrical statement: rather than saying $\partial_t^2 \Phi = -\omega^2 \Phi$, one can say $\xi(\xi(\Phi)) = -\omega^2 \Phi$. In other words, the frequencies come out right because the coordinates adapt themselves to the late-term stationarity. The process by which this adaptation occurs is, to our knowledge, still an open question.

At any rate, we must caution that this recovery of standard frequencies at late times should by no means be taken as license to overlook gauge ambiguity in numerical simulations. For example, it is quite tempting to associate the slight disagreement with perturbative results immediately after merger with nonlinear dynamics,

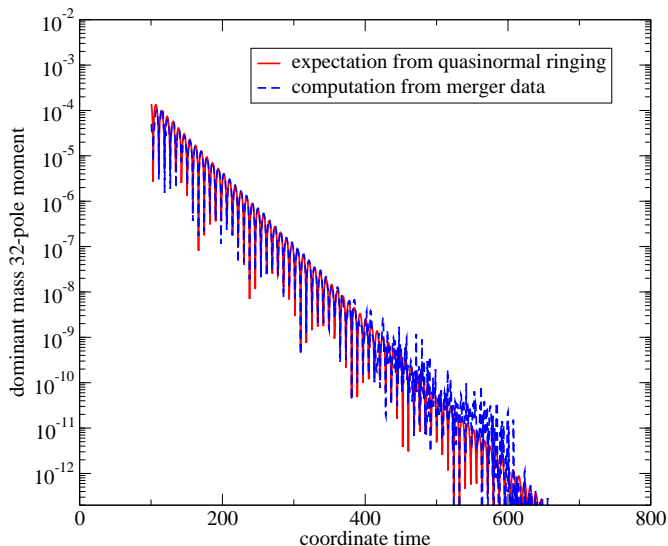


FIG. 13: Ringing of the dominant mass 32-pole moment as the product of a nonaxisymmetric head-on merger settles down to a Schwarzschild black hole.

however this disagreement could just as likely be due to the coordinates having not yet adapted to the approximate stationarity, or to stationarity simply not existing to a sufficient approximation. All of these effects (and perhaps others) will have an impact on the ringing immediately after merger, and a detailed investigation of the nonlinear extension of quasinormal ringing would require (at least partially) slicing-invariant comparisons beyond the scope of the current work. For example, one might treat the ringing of one multipole as a “clock” by which to measure the frequencies of the other multipoles.

IV. DISCUSSION

We have presented a definition of quasilocal source multipoles on dynamical horizons, adapted from that in Ref. [30] in such a way that it can be applied to horizons without axisymmetry, while preserving the agreement of the current dipole moment with the spin angular momentum defined by Hamiltonian methods [24]. More precisely, the vector spherical harmonics used to project out current multipoles are constructed in such a way that the dipole moment is identical to the spin angular momentum used in Ref. [22]. The key to this generalization is the definition of spherical harmonics as solutions to certain eigenvalue problems on the apparent horizon.

We have also applied this formalism to demonstrate that in a detailed and partially gauge-invariant sense, the binary black hole merger described in Ref. [4] indeed settles to a Kerr black hole, at least in the neighborhood of the horizon. There are limits to the gauge independence of this statement. The work here depends heavily on the formalism of dynamical horizons [25], which are de-

pendent on the slicing of spacetime (or, from a different viewpoint, are themselves invariantly defined yet carry unique foliations into apparent horizons that are compatible with the foliation of spacetime only in certain time slicings). Use of a unique and invariantly defined horizon such as the event horizon may be of interest (and is possible in the SpEC code [46]), however it would not alleviate the problem of slicing dependence, as a slicing must be chosen at some point to break the three-dimensional horizon worldtube into two-dimensional surfaces on which the spherical harmonic projections are taken.

A demonstration along the same lines as discussed here has been carried out before [31], however the numerical results here are somewhat stronger, and our generalization of the formalism has allowed the consideration of a non-axisymmetric merger.

Looking in detail at the ringdown of the multipoles, we have also recovered known quasinormal ringing frequencies. The dominant exponential damping timescale is recovered in the ringdown to Kerr geometry, and agrees with results from perturbation theory. Much more detailed results are found in the ringdown after a head-on collision leading to a Schwarzschild geometry, in which oscillation frequencies and damping timescales can be picked out mode by mode.

In future work we intend to study the ringdown of these datasets (and possibly others) on a local level, using a variant of the method presented in Ref. [36].

As for the multipole moments themselves, various avenues of investigation are open. The methods used here could be applied to study the tidal interaction of black holes during fully nonlinear binary inspiral and merger, including a full nonlinear generalization of certain results [41, 42] of black hole perturbation theory. As mentioned in Ref. [30], quasilocal source multipoles might also be applicable in trying to find a generalization, to exact general relativity, of Einstein’s celebrated quadrupole formula. Related to this, one might hope to recover force laws at the quasilocal level, relating black hole kicks to products of multipoles, as is done in the asymptotic regime in Ref. [17]. However, such an investigation would presumably require a satisfactory quasilocal definition of black hole linear momentum, which (if possible at all) appears to be beyond the realm of current understanding.

Acknowledgments

I heartily thank Mark Scheel, for providing the numerical simulation data from Ref. [4], and Geoffrey Lovelace, for the data from Ref. [45]. I also thank Saul Teukolsky and Larry Kidder for advice, on the project and on the manuscript. The work described here was supported by NSF grants PHY-0652952, DMS-0553677, and PHY-0652929; NASA grant NNX09AF96G, and a grant from the Sherman Fairchild Foundation.

-
- [1] F. Pretorius, Phys. Rev. Lett. **95**, 121101 (2005).
- [2] M. Campanelli, C. O. Lousto, P. Marronetti, and Y. Zlochower, Phys. Rev. Lett. **96**, 111101 (2006).
- [3] J. G. Baker, J. Centrella, D.-I. Choi, M. Koppitz, and J. van Meter, Phys. Rev. Lett. **96**, 111102 (2006).
- [4] M. A. Scheel, M. Boyle, T. Chu, L. E. Kidder, K. Matthews, and H. P. Pfeiffer, Phys. Rev. D **79**, 024003 (2009), arxiv:0810.1767.
- [5] M. Campanelli, C. O. Lousto, and Y. Zlochower, Phys. Rev. D **74**, 041501(R) (2006), gr-qc/0604012.
- [6] M. Campanelli, C. O. Lousto, Y. Zlochower, B. Krishnan, and D. Merritt, Phys. Rev. D **75**, 064030 (2007), gr-qc/0612076.
- [7] F. Herrmann, I. Hinder, D. Shoemaker, P. Laguna, and R. A. Matzner, Astrophys. J. **661**, 430 (2007), gr-qc/0701143.
- [8] M. Koppitz, D. Pollney, C. Reisswig, L. Rezzolla, J. Thornburg, P. Diener, and E. Schnetter, Phys. Rev. Lett. **99**, 041102 (2007), gr-qc/0701163.
- [9] M. Campanelli, C. O. Lousto, Y. Zlochower, and D. Merritt, Astrophys. J. Letters **659**, L5 (2007).
- [10] D.-I. Choi, B. J. Kelly, W. D. Boggs, J. G. Baker, J. Centrella, and J. van Meter, Phys. Rev. D **76**, 104026 (2007), gr-qc/0702016.
- [11] J. A. Gonzalez, M. D. Hannam, U. Sperhake, B. Brüggmann, and S. Husa, Phys. Rev. Lett. **98**, 231101 (2007), gr-qc/0702052.
- [12] M. Campanelli, C. O. Lousto, Y. Zlochower, and D. Merritt, Phys. Rev. Lett. **98**, 231102 (2007), gr-qc/0702133.
- [13] J. G. Baker, W. D. Boggs, J. Centrella, B. J. Kelly, S. T. McWilliams, M. C. Miller, and J. R. van Meter, Astrophys. J. **668**, 1140 (2007), astro-ph/0702390.
- [14] W. Tichy and P. Marronetti, Phys. Rev. D **76**, 061502 (2007), gr-qc/0703075.
- [15] F. Herrmann, I. Hinder, D. M. Shoemaker, P. Laguna, and R. A. Matzner, Phys. Rev. D **76**, 084032 (2007), arXiv:0706.2541v2.
- [16] B. Brüggmann, J. A. González, M. Hannam, S. Husa, and U. Sperhake, Phys. Rev. D **77**, 124047 (2008), arXiv:0707.0135.
- [17] J. D. Schnittman, A. Buonanno, J. R. van Meter, J. G. Baker, W. D. Boggs, J. Centrella, B. J. Kelly, and S. T. McWilliams, Phys. Rev. D **77**, 044031 (2008), arXiv:0707.0301v2.
- [18] J. G. Baker, W. D. Boggs, J. Centrella, B. J. Kelly, S. T. McWilliams, M. C. Miller, and J. R. van Meter, Astrophys. J. **682**, L29 (2008), arXiv:0802.0416.
- [19] S. H. Miller and R. Matzner, Gen. Relativ. Gravit. **41**, 525 (2009), 0807.3028.
- [20] J. Healy, F. Herrman, I. Hinder, D. M. Schoemaker, P. Laguna, and R. A. Matzner, Phys. Rev. Lett. **102**, 041101 (2009), arxiv:0807.3292.
- [21] S. Dain, C. O. Lousto, and Y. Zlochower, Phys. Rev. D **78**, 024039 (2008), arXiv:0803.0351v2.
- [22] G. Lovelace, R. Owen, H. P. Pfeiffer, and T. Chu, Phys. Rev. D **78**, 084017 (2008), arXiv:0805.4192.
- [23] J. D. Brown and J. W. York, Phys. Rev. D **47**, 1407 (1993).
- [24] A. Ashtekar, C. Beetle, and J. Lewandowski, Phys. Rev. D **64**, 044016 (2001), gr-qc/0103026.
- [25] A. Ashtekar and B. Krishnan, Phys. Rev. D **68**, 104030 (2003).
- [26] O. Dreyer, B. Krishnan, D. Shoemaker, and E. Schnetter, Phys. Rev. D **67**, 024018 (2003).
- [27] R. Owen, Ph.D. thesis, California Institute of Technology (2007), URL <http://resolver.caltech.edu/CaltechETD:etd-05252007-143511>.
- [28] G. B. Cook and B. F. Whiting, Phys. Rev. D **76**, 041501(R) (2007).
- [29] C. Beetle (2008), arXiv:0808.1745.
- [30] A. Ashtekar, J. Engle, T. Pawlowski, and C. Van Den Broeck, Class. Quantum Grav. **21**, 2549 (2004).
- [31] E. Schnetter, B. Krishnan, and F. Beyer, Phys. Rev. D **74**, 024028 (2006), gr-qc/0604015.
- [32] N. Vassetz, J. Novak, and J. L. Jaramillo, Phys. Rev. D **79**, 124010 (2009), arXiv:0901.2052.
- [33] M. Jasiulek (2009), arXiv:0906.1228.
- [34] H. Friedrich, I. Rácz, and R. M. Wald, Comm. Math. Phys. **204**, 691 (1999).
- [35] B. F. Whiting, J. Math. Phys. **30**, 1301 (1989).
- [36] M. Campanelli, C. O. Lousto, and Y. Zlochower, Phys. Rev. D **79**, 084012 (2009), arXiv:0811.3006.
- [37] E. Anderson, Z. Bai, C. Bischof, S. Blackford, J. Demmel, J. Dongarra, J. DuCroix, A. G. and S. Hammarling, A. McKenney, and D. Sorensen, *LAPACK Users' Guide* (Society for Industrial and Applied Mathematics, Philadelphia, 1999).
- [38] R. Penrose and W. Rindler, *Spinors and Space-Time: Vol. 1, Two-Spinor Calculus and Relativistic Fields* (Cambridge University Press, Cambridge, UK, 1987), ISBN 0521337070.
- [39] C. Gundlach, Phys. Rev. D **57**, 863 (1998).
- [40] K. S. Thorne, R. H. Price, and D. A. MacDonald, *Black Holes: The Membrane Paradigm* (Yale University Press, New Haven and London, 1986), 1st ed., ISBN 0-300-03770-8.
- [41] J. B. Hartle, Phys. Rev. D **9**, 2749 (1974).
- [42] H. Fang and G. Lovelace, Phys. Rev. D **72**, 124016 (2005).
- [43] E. W. Leaver, Proc. R. Soc. Lond. A **402**, 285 (1985).
- [44] S. Teukolsky, Astrophys. J. **185** (1973).
- [45] G. Lovelace, Y. Chen, M. Cohen, J. D. Kaplan, D. Koppel, K. D. Matthews, D. A. Nichols, M. A. Scheel, and U. Sperhake (2009), arXiv:0907.0869.
- [46] M. Cohen, H. P. Pfeiffer, and M. A. Scheel, Class. Quantum Grav. **26**, 035005 (2009), arXiv:0809.2628.